A novel macroscopic traffic model based on generalized optimal velocity model*

Zhou Xuan-Hao(周玄昊) and Lü Yong-Zai(吕勇哉)†

State Key Laboratory of Industrial Control Technology, Institute of Cyber-Systems and Control, Zhejiang University, Hangzhou 310027, *China*

(Received 27 April 2010; revised manuscript received 24 June 2010)

In this paper, we adopt the coarse graining method proposed by Lee H K *et al.* to develop a macroscopic model from the microscopic traffic model-GOVM. The proposed model inherits the parameter p which considers the influence of next-nearest car introduced in the GOVM model. The simulation results show that the new model is strictly consistent with the former microscopic model. Using this macroscopic model, we can avoid considering the details of each traffic on the road, and build more complex models such as road network model easily in the future.

Keywords: macroscopic model, microscopic model, traffic flow
PACS: 45.70.Vn **DOI:** 10.1088/1674-1056/20/1/014501

1. Introduction

The researches investigating the traffic flow have grown rapidly in recent years, not only to give support to the traffic guiding and assignment, but also to observe and analyse the nonlinear phenomenon and phase transition existing in the traffic flows. Among all these works, the major models used to describe the traffic flow can be classified into the following three catagories:[1]

Macroscopic model considers the macroscopic quantities such as velocity v and density ρ etc. It is usually represented by a system of partial differential equations consisting of a mass conservative equation and a dynamic equation. The original macroscopic model is the Lighthill–Whitham model.[2] After that, Payne–Whitham model was proposed considering the car-following theory and its general form is

$$\begin{cases} \dfrac{\partial \rho}{\partial t} + \dfrac{\partial(\rho v)}{\partial x} = 0, \\ \dfrac{\partial v}{\partial t} + v\dfrac{\partial v}{\partial x} = \underbrace{-\dfrac{1}{T}(v - V_{\mathrm{e}}(\rho))}_{\text{relaxation term}} - \underbrace{\dfrac{c^2(\rho)}{\rho}\dfrac{\partial \rho}{\partial x}}_{\text{anticipation term}}, \end{cases} \tag{1}$$

here T is the relaxation time, V_{e} is the optimal velocity function, and c is the anticipation function associated with density ρ. Many variants of this model were devclored, such as those in the Refs. [3] and [4]. Furthermore, a small diffusion term is often added to the Payne–Whitham model to smooth the wave fronts, such as KK model proposed by Kerner and Konhäuser in Ref. [5]. The macroscopic model has following advantages: (i) good agreement with empirical data and clear description of many traffic flow phenomena (e.g. stop and go waves, congestions); (ii) suitability for analytical investigations due to the compact formulation; and (iii) extension of one-lane models to multilane models by considering a certain probability of overtaking or by other methods.[6]

Microscopic model considers each car's behaviour. The classical microscopic model contains CA (cellular automation),[7] car-following model, and their modifications. Optimal velocity model (OVM)[8] is an important class of car-following models whose typical form is as follows:

$$\frac{\mathrm{d}u_n(t)}{\mathrm{d}t} = \lambda(V(\Delta y_n(t)) - u_n(t)), \tag{2}$$

here $y_n(t), u_n(t)$ are the coordinate and velocity of the nth vehicle at time t. Thus the left side is the acceleration term of car n. The term $V(\Delta y_n(t))$ means the desired velocity depends on the headway between two cars (here V is an optimal velocity function). So the term $V(\Delta y_n(t)) - u_n(t)$ means the velocity difference needed to be reduced and λ is the sensitivity equal to the reciprocal of relax time. Many researches extended the model by considering more information from the system such as Refs. [9], [10], and [11]. In Ref. [12], the author gave a general model which considers the influence of the second-nearest car with the

*Project supported by National Creative Research Groups Science Foundation of China (Grant No. 60721062), National Basic Research Program of China (Grant No. 2007CB714000).
†Corresponding author. E-mail: yongzailu@yahoo.com
© 2011 Chinese Physical Society and IOP Publishing Ltd

form

$$\frac{\mathrm{d}u_n(t)}{\mathrm{d}t} = \lambda(V(\Delta y_n(t) + \Delta y_{n+1}(t)) - u_n(t)). \quad (3)$$

This model is named general optimal velocity model (GOVM), and the linear analysis was also given.

Gas kinetic model which often contains Boltzmann-like term, Dirk Helbing *et al.* in Ref. [13] gave a detailed description of this model. This model is the bridge between the macroscopic and the microscopic models.

In Refs. [14] and [11], the authors demonstrated the relationship between macroscopic model and microscopic model. However, the parameters in anticipation and dissipation terms aforementioned are always assigned by simulation or experience. In this paper, we adopt the coarse graining approach in Ref. [15] to build the macroscopic model directly from the GOVM. According to the above approach, we can quantitatively derive parameters in anticipation and dissipation terms based on the microscopic model. The linear analysis and simulation result show that macroscopic model is consistent with microscopic model strictly and the stable region is enlarged by inducing the influence of second-nearest car in both models.

The outline of this research is as follows: In Section 2, we will build the macroscopic model directly from GOVM model and the linear analysis will be given. The simulations and comparison will be presented in Section 3. Finally, we will make the conclusion in Section 4.

2. Build the macroscopic model

Here we consider a one-dimensional traffic flow problem. The nodes are defined as follows:

$y_n(t), n \in 1, 2, \ldots, N$: the coordinate of the nth vehicle at time t, here N is the number of traffic vehicles distributed on this road (associated with the microscopic model);

$x(t)$: the continuous distance coordinate after using coarse graining method (associated with the macroscopic model).

A natural way to obtain macroscopic description is to coarse grain these fields. As provided in Ref. [15], a coarse graining envelope function $\phi(x,t)$ which is non-negative valued is introduced. Its peak is located at $(x,t) = (0,0)$, and normalised as $\int \mathrm{d}x\mathrm{d}t\phi(x,t) = 1$. The coarse grained density $\rho(x,t)$ and flux $q(x,t)$ can be defined as in Ref. [15]:

$$\rho(x,t) = \int \mathrm{d}x'\mathrm{d}t'\phi(x-x',t-t')\hat{\rho}(x',t'), \quad (4)$$

$$q(x,t) = \int \mathrm{d}x'\mathrm{d}t'\phi(x-x',t-t')\hat{q}(x',t'), \quad (5)$$

here two microscopic field variables, density field $\hat{\rho}(x,t)$ and flux field $\hat{q}(x,t)$, are defined as:

$$\hat{\rho}(x,t) \equiv \sum_n \delta(y_n(t) - x), \quad (6)$$

$$\hat{q}(x,t) \equiv \sum_n \dot{y}_n(t)\delta(y_n(t) - x). \quad (7)$$

Obviously, we can obtain another coarse grained variable $v(x,t) = q(x,t)/\rho(x,t)$ to represent the field velocity easily.

Using lengthy partial integral, the equations that govern the time evolution of $\rho(x,t)$ and $q(x,t)$ are derived:

$$\frac{\partial\rho}{\partial t} + \frac{\partial(\rho v)}{\partial x} = 0, \quad (8)$$

$$\frac{\partial}{\partial t}q(x,t) = \rho(x,t)\langle\ddot{y}_n(t')\rangle_{(x,t)} - \frac{\partial}{\partial x}[\rho(x,t)\langle\dot{y}_n(t')\rangle_{(x,t)}]. \quad (9)$$

It is obviously that the Eq. (8) is identical with the classic fluid conservation equation. We rewrite Eq. (9) in terms of ρ and v instead of ρ and q correspondingly,

$$\rho\left(\frac{\partial v}{\partial t} + v\frac{\partial v}{\partial x}\right) = \rho\langle\ddot{y}_n(t')\rangle - \frac{\partial}{\partial x}(\rho\theta), \quad (10)$$

here

$$\theta(x,t) \equiv \langle\dot{y}_n^2(t')\rangle - v^2(x,t).$$

This Eq. (10) is similar to the momentum equation in common macroscopic model. By combining Eqs. (8) and (10) we can build a bridge between microscopic and macroscopic models.

2.1. From GOVM model

Based on the GOVM model[12] aforementioned by Eq. (3), we also assume,

$$V(\Delta y_n(t), \Delta y_{n+1}(t)) = (1-p)V(\Delta y_n(t)) + pV(\Delta y_{n+1}(t)). \quad (11)$$

The coarse graining of dynamic equation in GOVM leads to

$$\langle\ddot{y}_n\rangle = \lambda[\langle V(\Delta y_n, \Delta y_{n+1})\rangle - v]. \quad (12)$$

Here, we substitute the average variable v for the corresponding microscopic variable $u_n(t)$ directly, and the term $V(\Delta y_n(t), \Delta y_{n+1}(t))$ is also replaced by the mean value $\langle V(\Delta y_n, \Delta y_{n+1})\rangle$. The expansion of $\langle V(\Delta y_n, \Delta y_{n+1})\rangle$ with respect to $\langle \Delta y_n(t)\rangle, \langle \Delta y_{n+1}(t)\rangle$ is as follows:

$$\begin{aligned}\langle V(\Delta y_n, \Delta y_{n+1})\rangle &= \langle (1-p)V(\Delta y_n(t)) + pV(\Delta y_{n+1}(t))\rangle \\ &= (1-p)\sum_{m=0}^{\infty}\frac{1}{m!}V^{(m)}(\langle \Delta y_n\rangle)\langle(\Delta y_n - \langle \Delta y_n\rangle)^m\rangle \\ &\quad + p\sum_{m=0}^{\infty}\frac{1}{m!}V^{(m)}(\langle \Delta y_{n+1}\rangle)\langle(\Delta y_{n+1} - \langle \Delta y_{n+1}\rangle)^m\rangle \\ &\equiv (1-p)V(\langle \Delta y_n\rangle) + pV(\langle \Delta y_{n+1}\rangle) + \sum_{m=2}^{\infty}(I_m + I'_m). \end{aligned} \tag{13}$$

It is naturally to use $1/\rho(x,t)$ to express the distance between the car at the position x and its front car. But as pointed out in Ref. [15], the direction influence should been taken into consideration, so we use the density at middle point between point y_n and y_{n+1}, the middle point between point y_{n+1} and y_{n+2} to approximate the $\langle \Delta y_n\rangle_{(x,t)}$ and $\langle \Delta y_{n+1}\rangle_{(x,t)}$ as follows:

$$\begin{aligned}\langle \Delta y_n\rangle_{(x,t)} &\approx \rho^{-1}(x + 1/(2\rho(x,t)), t) \\ &= \rho^{-1} + \frac{1}{2\rho}\frac{\partial \rho^{-1}}{\partial x} + \Sigma_1, \\ \langle \Delta y_{n+1}\rangle_{(x,t)} &\approx \rho^{-1}(x + 3/(2\rho(x,t)), t) \\ &= \rho^{-1} + \frac{3}{2\rho}\frac{\partial \rho^{-1}}{\partial x} + \Sigma_2. \end{aligned} \tag{14}$$

Then, we get:

$$\begin{aligned} V(\langle \Delta y_n\rangle) &\approx V(\rho^{-1}) + V'(\rho^{-1})\left[\frac{1}{2\rho}\frac{\partial(\rho^{-1})}{\partial x}\right], \\ V(\langle \Delta y_{n+1}\rangle) &\approx V(\rho^{-1}) + V'(\rho^{-1})\left[\frac{3}{2\rho}\frac{\partial(\rho^{-1})}{\partial x}\right]. \end{aligned} \tag{15}$$

Combining Eqs. (10), (12), (13) and (15), we omit the second term in Eq. (10) which arises from the coarse graining process,

$$\begin{aligned}\frac{\partial v}{\partial t} + v\frac{\partial v}{\partial x} &= \langle \ddot{y}_n(t)\rangle \\ &= \lambda[\langle (V(\Delta(y_n, y_{n+1})\rangle - v] \\ &\simeq \lambda[(1-p)V(\langle \Delta y_n\rangle) + pV(\langle \Delta y_{n+1}\rangle) - v] \\ &= \lambda\left[(1-p)\left\{V(\rho^{-1}) + V'(\rho^{-1})\left[\frac{1}{2\rho}\frac{\partial(\rho^{-1})}{\partial x}\right]\right\} + p\left\{V(\rho^{-1}) + V'(\rho^{-1})\left[\frac{3}{2\rho}\frac{\partial(\rho^{-1})}{\partial x}\right]\right\} - v\right] \\ &= \lambda[V(\rho^{-1}) - v] + \frac{\lambda(1+2p)}{2\rho}V'(\rho^{-1})\frac{\partial \rho^{-1}}{\partial x}. \end{aligned} \tag{16}$$

2.2. Linear analysis

The small perturbations with respect to the homogeneous state in the GOVM model can be written as:

$$y_n(t) = v_h t + \rho_h^{-1} n + \delta x \exp(\mathrm{i}\,\kappa n + \gamma t). \tag{17}$$

Here the third term at the right side is the perturbations and δx is the amplitude, γ is the frequency measured in the reference frame moving with the velocity v_h. Using the linear analysis method proposed in Ref. [8], we get the solution for the variable γ,

$$\gamma_{\pm} = \frac{\lambda}{2}\left[-1 \pm \sqrt{1 + \frac{4V'}{\lambda}(\mathrm{e}^{\mathrm{i}\,\kappa} - 1)(p\mathrm{e}^{\mathrm{i}\,\kappa} + 1 - p)}\right], \tag{18}$$

where $V' = V'(\rho_h^{-1})$. We expand γ as

$$\gamma = \gamma_1(\mathrm{i}\,\kappa) + \gamma_2(\mathrm{i}\,\kappa)^2 + \cdots. \tag{19}$$

Omit the high-order terms, we obtain the stability region in the linear regime as:

$$V'(\Delta y_n) < \frac{\lambda}{2}(1+2p). \tag{20}$$

Compared with the stability region $V'(\Delta y_n) < \lambda/2$ in optimal velocity model, it is shown that we can enlarge the stable region by introducing the factor of the influence p of the next-nearest car as pointed out in Ref. [9].

On the other hand, small perturbations in the macroscopic model can be written as

$$\rho(x,t) = \rho_h + \delta\rho \exp(\mathrm{i}\, kx + \omega t),$$
$$v(x,t) = v_h + \delta v \exp(\mathrm{i}\, kx + \omega t). \quad (21)$$

Linearising the Eqs. (8) and (16), we derive:

$$\omega\delta\rho + \rho_h \cdot (\mathrm{i}\, k) \cdot \delta v + v_h \cdot (\mathrm{i}\, k) \cdot \delta\rho = 0$$
$$\Rightarrow \delta\rho = -\frac{\mathrm{i}\, k\rho_h}{\omega + \mathrm{i}\, kv_h}\delta v, \quad (22)$$

and

$$(\omega + \mathrm{i}\, kv_h)\delta v = -\lambda V'(\rho_h^{-1}) \cdot \rho_h^{-2}\delta\rho(1 + \frac{1}{2}\,\mathrm{i}\, k\rho_h^{-1}) - \lambda\delta v - \lambda p V'(\rho_h^{-1}) \cdot \rho_h^{-3} \cdot \delta\rho \cdot \mathrm{i}\, k. \quad (23)$$

Substituting Eq. (22) for the corresponding terms in Eq. (23), it can be reduced to:

$$\begin{aligned}(\omega + \mathrm{i}\, kv_h)^2 &= \lambda V'(\rho_h^{-1}) \cdot \rho_h^{-2} \cdot \mathrm{i}\, k\rho_h \cdot \left(1 + \frac{1}{2}\,\mathrm{i}\, k\rho_h^{-1}\right) + \lambda(\omega + \mathrm{i}\, kv_h) + \lambda p V'(\rho_h^{-1})\rho_h^{-3} \cdot (\mathrm{i}\, k)^2\rho_h \\ &\Rightarrow (\omega + \mathrm{i}\, kv_h)^2 + \lambda(\omega + \mathrm{i}\, kv_h) - \lambda V'(\rho_h^{-1})(\mathrm{i}\, k\rho_h^{-1} + \frac{1}{2}(1+2p)(\mathrm{i}\, k\rho_h^{-1})^2) = 0 \\ &\Rightarrow \omega_\pm + \mathrm{i}\, kv_h = \frac{\lambda}{2}\left[-1 \pm \sqrt{1 + \frac{4V'}{\lambda}(\mathrm{i}\, k\rho_h^{-1} + \frac{1}{2}(1+2p)(\mathrm{i}\, k\rho_h^{-1})^2)}\right]. \end{aligned} \quad (24)$$

If we expand the second term inside the radical sign in Eq. (16), it turns to:

$$\gamma_\pm = \frac{\lambda}{2}\left[-1 \pm \sqrt{1 + \frac{4V'}{\lambda}(\mathrm{e}^{\mathrm{i}\,\kappa} - 1)(p\mathrm{e}^{\mathrm{i}\,\kappa} + 1 - p)}\right] \approx \frac{\lambda}{2}\left[-1 \pm \sqrt{1 + \frac{4V'}{\lambda}(\mathrm{i}\,\kappa + \frac{1}{2}(1+2p)(\mathrm{i}\,\kappa)^2)}\right]. \quad (25)$$

Comparing Eq. (24) with Eq. (25), it is obvious that κ corresponds to $\omega + \mathrm{i}\, kv_h$. In Ref. [15], the author indicated that the kp_h^{-1} is the macroscopic counterpart of κ, both representing the phase difference between two successive vehicles. Thus it is clear that the macroscopic momentum equation with the continuity equation can describe the long wave-length behavior of microscopic model exactly in the linear regime.

3. Simulation

In this section, the simulations on both microscopic and macroscopic models are made. Here we mainly assume a cycle road where all cars are distributed homogeneous with little perturbation on the road initially. The same initial condition and parameters are assigned as in Ref. [15]. A system size $L = 2.33$ km is simulated with N vehicles ($\rho_h = N/L$), and the following microscopic initial conditions are used:

$$\begin{aligned} y_n(0) &= n\rho_h^{-1} + A\sin(6\pi n\rho_h^{-1}/L), \\ &\quad 1 \leqslant n < N/3, \\ y_n(0) &= n\rho_h^{-1}, \quad N/3 \leqslant n \leqslant N, \\ \dot{y}_n(0) &= V(\Delta y_n(0)), \quad \text{for all } n, \end{aligned} \quad (26)$$

and the system obeys the periodic condition. The optimal velocity function

$$V(\Delta y_n) = \frac{v_{\max}}{2}\left[\tanh\left(2\frac{\Delta y_n - x_{\text{neutral}}}{x_{\text{width}}}\right) + c_{\text{bias}}\right] \quad (27)$$

with $v_{\max} = 33.6$ m/s, $x_{\text{neutral}} = 25$ m, $x_{\text{width}} = 23.3$ m, $c_{\text{bias}} = 0.913$, and $\lambda = 2\ \text{s}^{-1}$. Comparisons are made to verify the validity of the macroscopic model.

3.1. Microscopic simulation

We use Eular method which approximately describes the velocity and location of each car as follows.

$$\dot{y}_n(t + \Delta t) = \dot{y}_n(t) + \ddot{y}_n(t)\Delta t,$$
$$y_n(t + \Delta t) = y_n(t) + \dot{y}_n(t)\Delta t + \frac{1}{2}\ddot{y}_n(t)(\Delta t)^2. \quad (28)$$

In our simulation we use $\Delta t = 0.001$ s, and the linear stability analysis gives the unstable region as shown in Table 1.

Table 1. The critical stability conditions for different value p.

p	0	0.1	0.2	0.3
unstable area	[73, 130]	[75, 124]	[78, 116]	[81, 109]

3.2. Macroscopic simulation

Firstly, if we deeply investigate into Eq. (14), the second order terms Σ_1, Σ_2 can be derived as,

$$\Sigma_1 = \frac{1}{6\rho^2}\frac{\partial^2\rho^{-1}}{\partial x^2},$$
$$\Sigma_2 = \frac{3}{8\rho^2}\frac{\partial^2\rho^{-1}}{\partial x^2}. \tag{29}$$

Equation (30) can be developed to replace the Eq. (16) where the second second-order differential term is introduced.

$$\frac{\partial v}{\partial t} + v\frac{\partial v}{\partial x} = \lambda[V(\rho^{-1}) - v] + \frac{\lambda(1+2p)}{2\rho}V'(\rho^{-1})\frac{\partial\rho^{-1}}{\partial x} + \frac{\lambda(1+\frac{5}{4}p)}{6\rho^2}\frac{\partial^2 v}{\partial x^2}. \tag{30}$$

It is well known that the conservative scheme is a good choice for carrying out numerical tests if dynamics model is used to describe traffic flow. As we know, the character of N–S equation with viscosity term can be classified to the mixture of ellipse and parabola. We use MacCormack iteration method to get the numeric solution of this viscosity equation. Each step of iteration contains two substeps called prediction and calibration as follows:

Prediction: Use forward difference to discretize the space corresponding to the equations,

$$\left(\frac{\partial\rho}{\partial t}\right)_i^t = -\left(\rho_i^t\frac{v_{i+1}^t - v_i^t}{\Delta x} + v_i^t\frac{\rho_{i+1}^t - \rho_i^t}{\Delta x}\right), \tag{31}$$

$$\left(\frac{\partial v}{\partial t}\right)_i^t = -\left(v_i^t\frac{v_{i+1}^t - v_i^t}{\Delta x} - \lambda(V((\rho_i^t)^{-1}) - v_i^t) + \frac{\lambda(1+2p)}{2(\rho_i^t)^3}V'((\rho_i^t)^{-1})\frac{\rho_{i+1}^t - \rho_i^t}{\Delta x} - \frac{\lambda(1+\frac{5}{4}p)}{6(\rho_i^t)^2}\frac{v_{i+1}^t + v_{i-1}^t - 2v_i^t}{\Delta x^2}\right). \tag{32}$$

Then we get the predictive value of $\rho_i^{t+\Delta t}$ and $v_i^{t+\Delta t}$ which mean the density and velocity at time $t+\Delta t$, respectively,

$$(\bar{\rho})_i^{t+\Delta t} = \rho_i^t + \left(\frac{\partial\rho}{\partial t}\right)_i^t\Delta t,$$
$$(\bar{v})_i^{t+\Delta t} = v_i^t + \left(\frac{\partial v}{\partial t}\right)_i^t\Delta t. \tag{33}$$

Calibration: Use backward difference and predictive value obtained,

$$\left(\frac{\bar{\partial}\rho}{\partial t}\right)_i^{t+\Delta t} = -\left[(\bar{\rho})_i^{t+\Delta t}\frac{(\bar{v})_i^{t+\Delta t} - (\bar{v})_{i-1}^{t+\Delta t}}{\Delta x} + (\bar{v})_i^{t+\Delta t}\frac{(\bar{\rho})_i^{t+\Delta t} - (\bar{\rho})_{i-1}^{t+\Delta t}}{\Delta x}\right]. \tag{34}$$

And we can get $\left(\bar{\partial v}/\partial t\right)_i^{t+\Delta t}$ similar to Eqs. (32) and (34). Then we get the average value of one order

$$\left(\frac{\partial\rho}{\partial t}\right)_{\rm av} = \frac{1}{2}\left[\left(\frac{\partial\rho}{\partial t}\right)_i^t + \left(\frac{\bar{\partial}\rho}{\partial t}\right)_i^{t+\Delta t}\right]. \tag{35}$$

Finally, we get the calibrated value of ρ at time $t+\Delta t$ using

$$\rho_i^{t+\Delta t} = \rho_i^t + \left(\frac{\partial\rho}{\partial t}\right)_{\rm av}\Delta t, \tag{36}$$

where i, n, $\Delta x = 1$ m, and $\Delta t = 0.001$ s are the space and time indices, and the spatial and time steps, respectively. So we can use the above method to get the new state at time $t+1$ based on the information at time t. Thus we can make the iteration from the initial condition to the final state.

3.3. Comparison

We change the number of cars N and the factor p to make a series of simulations. The simulation results are shown in Figs. 1 to 5.

Through these figures, we can conclude that:

(i) In all figures, we can see the solid lines which represent the velocity distribution on the road match up the trend of the points very well. It indicates that the macroscopic model can describe the dynamic character of traffic flow almost identically with the GVOM model.

(ii) As shown in Figs. 1, 2, 4, and 5, with the factor p increased, at the same time when $t = 10$ min or $t = 30$ min, the amplitude of the velocity wave with $p = 0.2$ are much smaller than that with $p = 0.1$. It indicates that the stability of the system is enhanced with the increase of the factor p.

(iii) If the value of p is in the unstable region as shown in Fig. 3, the macroscopic model gets a less accurate result than in the stable case.

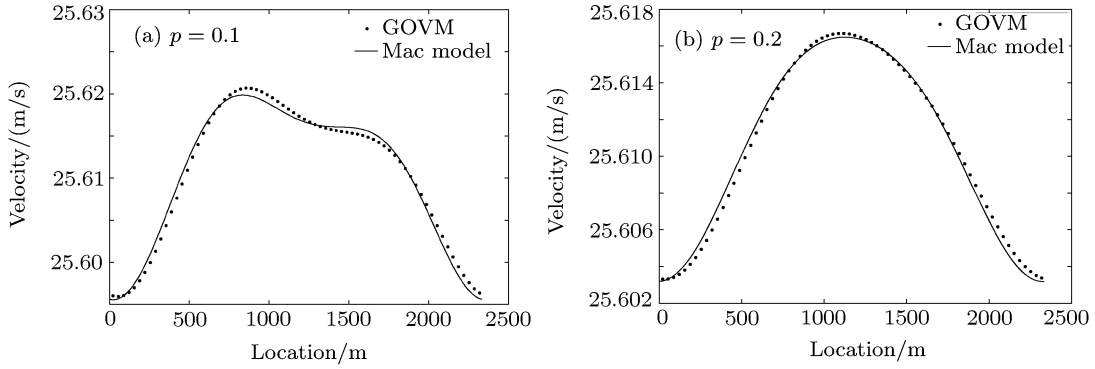


Fig. 1. When $N = 70$, $t = 10$ min.

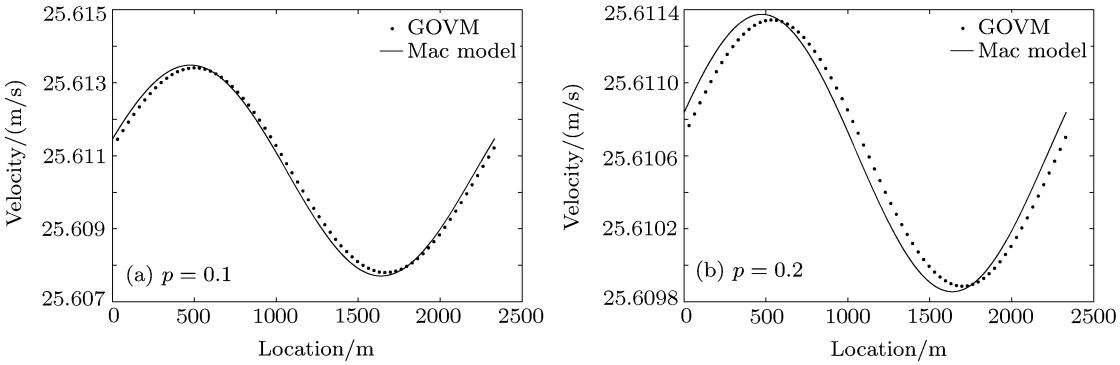


Fig. 2. When $N = 70$, $t = 30$ min.

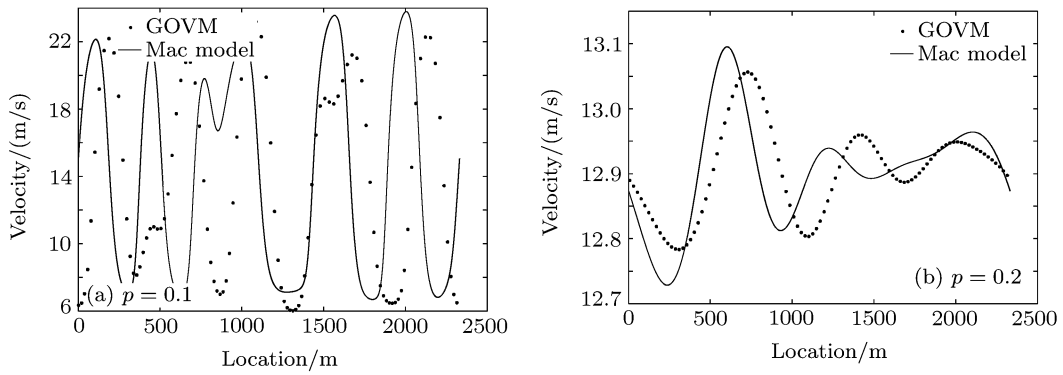


Fig. 3. When $N = 100$, $t = 10$ min.

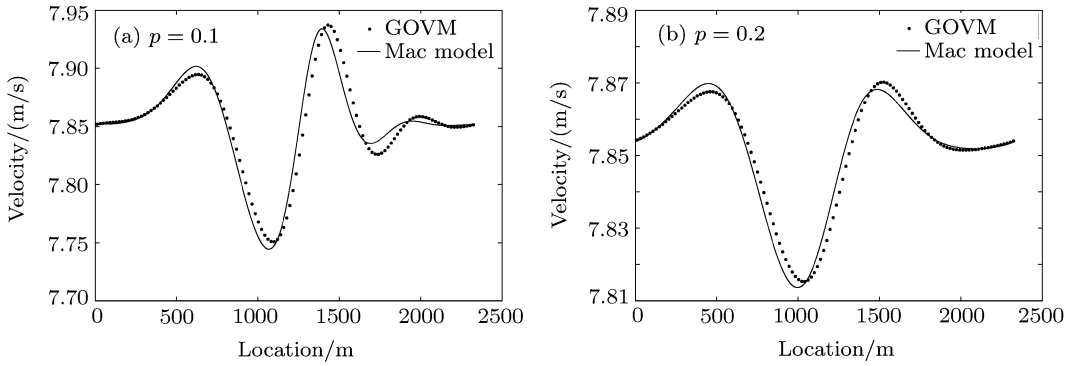


Fig. 4. When $N = 120$, $t = 10$ min.

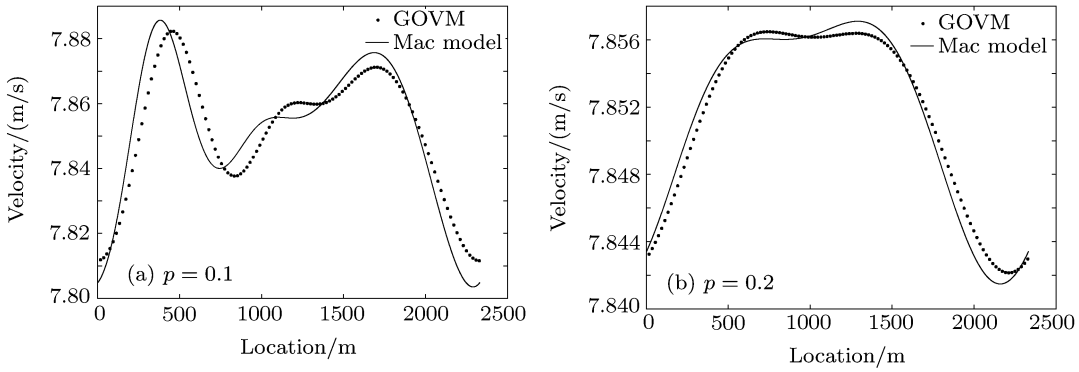


Fig. 5. When $N = 120$, $t = 30$ min.

3.4. Deviant analysis

Secondly, we calculate the deviation in the following expression between the two models, and the results are given in Table 2.

$$d_v(t) \equiv \frac{\sqrt{\langle [v_{\text{macro}}(x,t) - v_{\text{micro}}(x,t)]^2 \rangle_{\text{space}}}}{\langle v_{\text{micro}}(x,t) \rangle_{\text{space}}}. \tag{37}$$

Table 2. The variance analysis between the macroscopic model and GOVM microscopic model.

p	$N = 70, t = 10$	$N = 70, t = 30$	$N = 100, t = 10$	$N = 120, t = 10$	$N = 120, t = 30$
0.1	0.086%	0.045 %	$\gg 100$ %	0.53 %	0.77%
0.2	0.032%	0.012 %	8.36 %	0.4%	0.3%

This table shows that except the unstable cases when $N = 100$, the deviant between the macroscopic model and the GOVM model is below the level of 1%. The results prove that our new macroscopic model derived from GOVM is successful in depicting the traffic flow.

4. Conclusion

In this paper, we adopted the coarse graining method proposed in Ref. [15] to get a macroscopic model from GOVM. By the simulation, we demonstrated that the macroscopic model exactly describes the traffic flow and is consistent with the GOVM model. We can enhance the stability of the system by increasing the influence factor p, both in macroscopic model and microscopic model.

References

[1] Dirk Helbing 2001 *Rev. Mod. Phys.* **73** 1067

[2] Lighthill M J and Whitham G B 1955 *Proc. Roy. Soc.* A **229** 28

[3] Zhang H M 2003 *Transportation Research* B **37** 27

[4] Tang T Q, Li Y and Huang H J 2009 *Int. J. Mod. Phys.* C **20** 941

[5] Kerner B S and Konhäuser P 1993 *Phys. Rev.* E **48** 2335

[6] Tang C F, Jiang R and Wu Q S 2007 *Chin. Phys.* **16** 1570

[7] Codd E F 1968 *Cellular Automata* (New York: Academic Press)

[8] Banda M, Hasebe K, Nakayam A and Sugiyama Y 1995 *Phys. Rev.* E **51** 1035

[9] Li Z P and Liu Y C 2007 *Int. J. Mod. Phys.* C **18** 819

[10] Peng G H and Sun D H 2009 *Chin. Phys.* B **18** 5420

[11] Li Z P and Liu Y C 2007 *Traffic Flow Modeling and Traffic Status Analysis for City Road Network* Ph.D. dissertation (Shanghai: Shanghai Jiao Tong University)

[12] Sawada Shiro 2001 *J. Phys.* A: *Math. Gen* **34** 11253

[13] Dirk Helbing 1996 *Phys. Rev.* E **53** 2366

[14] Jiang R, Wu Q S and Zhu Z J 2001 *Chin. Sci. Bull.* **46** 345

[15] Lee H K, Lee H W and Kim D 2001 *Phys. Rev.* E **64** 056126